J|A|C|S
ARTICLES

Published on Web 11/01/2008

Synthesis of a Dialuminum-Substituted Silicotungstate and the Diastereoselective Cyclization of Citronellal Derivatives

Yuji Kikukawa, Syuhei Yamaguchi, Yoshinao Nakagawa, Kazuhiro Uehara, Sayaka Uchida, Kazuya Yamaguchi, and Noritaka Mizuno*

Department of Applied Chemistry, School of Engineering, The University of Tokyo, 7-3-1 Hongo, Bunkyo-ku, Tokyo 113-8656, Japan

Received February 26, 2008; Revised Manuscript Received July 31, 2008; E-mail: tmizuno@mail.ecc.u-tokyo.ac.jp

Abstract: A novel dialuminum-substituted silicotungstate $TBA_3H[\gamma\text{-}SiW_{10}O_{36}\{Al(OH_2)\}_2(\mu\text{-}OH)_2]\cdot 4H_2O$ (**1**, TBA = tetra-*n*-butylammonium) was synthesized by the reaction of the potassium salt of $[\gamma\text{-}SiW_{10}O_{36}]^{8-}$ (**SiW10**) with 2 equiv of $Al(NO_3)_3$ in an acidic aqueous medium. It was confirmed by the X-ray crystallographic analysis that compound **1** was a monomer of the γ-Keggin dialuminum-substituted silicotungstate with the $\{Al_2(\mu\text{-}OH)_2\}$ diamond core. The cluster framework of **1** maintained the γ-Keggin structure in the solution states. The reaction of **1** with pyridine yielded $TBA_3[(C_5H_5N)H][\gamma\text{-}SiW_{10}O_{36}\{Al(C_5H_5N)\}_2(\mu\text{-}OH)_2]\cdot 2H_2O$ (**2**), and the molecular structure was successfully determined by the X-ray crystallographic analysis. In compound **2**, two of three pyridine molecules coordinated to the axial positions of aluminum centers and one of them existed as a pyridinium cation, showing that compound **1** has two Lewis acid sites and one Brønsted acid site. Compound **1** showed high catalytic activity for the intramolecular cyclization of citronellal derivatives such as (+)-citronellal (**3**) and 3-methylcitronellal (**4**) without formation of byproduct resulting from etherification and dehydration. For the **1**-catalyzed cyclization of **3**, the diastereoselectivity toward (−)-isopulegol (**3a**) reached ca. 90% and the value was the highest level among those with reported systems so far. The reaction rate for the **1**-catalyzed cyclization of **3** decreased by the addition of pyridine, and the cyclization hardly proceeded in the presence of 2 equiv of pyridine with respect to **1**. On the other hand, the reaction rate and diastereoselectivity to **3a** in the presence of 2,6-lutidine were almost the same as those in the absence. Therefore, the present cyclization is mainly promoted by the Lewis acid sites (aluminum centers) in **1**. DFT calculations showed that the formation of the transition state to produce **3a** is sterically and electronically more favorable than the other three transition states for the present **1**-catalyzed cyclization of **3**.

Introduction

Polyoxometalates are a large family of anionic metal−oxygen clusters of early transition metals and have stimulated many current research activities in broad fields of science such as catalysis, materials, and medicine, because their chemical properties such as redox potentials, acidities, and solubilities in various media can be finely tuned by choosing constituent elements and counter cations.[1] Particularly, the interest in the catalysis of metal-substituted polyoxometalates, which are synthesized by the substitution of metal cations into the vacant site(s) of lacunary polyoxometalates as "structural motifs", has been growing because of the rich diversity of lacunary polyoxometalates, ranging from monovacant to hexavacant anions.[1] Although polyoxometalates have been traditionally used as Brønsted acid and oxidation catalysts, there are only a few reports on the Lewis acid catalysis by polyoxometalates.[2] The Lewis acid catalysis of polyoxometalates is a promising new avenue for the polyoxometalate chemistry and lanthanoid-substituted polyoxometalates $[\alpha_1\text{-}Ln(H_2O)_4P_2W_{17}O_{61}]^{7-}$ (Ln = La, Sm, Eu, and Yb), and hafnium-substituted polyoxometalates such as $[\alpha_1\text{-}Hf(H_2O)_nP_2W_{17}O_{61}]^{6-}$ and $[\alpha\text{-}Hf(OH)PW_{11}O_{39}]^{4-}$ have been reported to act as Lewis acid catalysts for imine aldol and imino Diels−Alder reactions, for example.[2]

Aluminum cations are naturally electron-deficient, and their derivatives with the weakly coordinating ligands behave as coordinatively unsaturated compounds.[3] In particular, aluminum compounds are very useful Lewis acid catalysts.[3] Since the properties and reactivities are strongly dependent on their structures, the syntheses of aluminum compounds with structurally well-defined sites are very important. While some kinds of aluminum-substituted polyoxometalates such as mono- and trisubstituted Keggin heteropolytungstates (not γ-type), mono-

(1) (a) Hill, C. L.; Prosser-McCartha, C. M. *Coord. Chem. Rev.* **1995**, *143*, 407. (b) Okuhara, T.; Mizuno, N.; Misono, M. *Adv. Catal.* **1996**, *41*, 113. (c) Neumann, R. *Prog. Inorg. Chem.* **1998**, *47*, 317. (d) Thematic issue on polyoxometalates. Hill, C. L. *Chem. Rev.* **1998**, *98*, 1−390. (e) Kozhevnikov, I. V. *Catalysis by Polyoxometalates*; John Wiley & Sons, Ltd.: Chichester, 2002. (f) Mizuno, N; Yamaguchi, K.; Kamata, K. *Coord. Chem. Rev.* **2005**, *249*, 1944.

(2) (a) Boglio, C.; Lemiére, G.; Hasenknopf, B.; Thorimbert, S.; Lacôte, E.; Malacria, M. *Angew. Chem., Int. Ed.* **2006**, *45*, 3324. (b) Boglio, C.; Micoine, K.; Rémy, P.; Hasenknopf, B.; Thorimbert, S.; Lacôte, E.; Malacria, M.; Afonso, C.; Tabet, J.-C. *Chem. Eur. J.* **2007**, *13*, 5426.

(3) (a) Ooi, T.; Maruoka, K. In *Lewis Acids in Organic Synthesis*; Yamamoto, H., Eds.; Wiley-VCH: Weinheim, 2000; pp 191−281. (b) Wulff, W. D. In *Lewis Acids in Organic Synthesis*; Yamamoto, H., Eds.; Wiley-VCH: Weinheim, 2000; pp 283−354. (c) Saito, S. In *Main Group Metals in Organic Systhesis*; Yamamoto, H., Oshima, K., Eds.; Wiley-VCH: Weinheim, 2004, pp 189−306.

10.1021/ja8014154 CCC: $40.75

substituted Wells−Dawson heteropolytungstates, and a trisubstituted β-Keggin silicotungstate dimer have been synthesized by using lacunary polyoxometalates as "structural motifs",[4] structurally characterized aluminum-substituted polyoxometalates (by X-ray crystallographic analysis) are still one of the least reported compounds.[4] In this paper, we report the synthesis, structural characterization, and Lewis acid catalysis of a novel dialuminum-substituted γ-Keggin-type silicotungstate $TBA_3H[\gamma\text{-}SiW_{10}O_{36}\{Al(OH_2)\}_2(\mu\text{-}OH)_2]\cdot 4H_2O$ (**1**, TBA = tetra-*n*-butylammonium).

Results and Discussion

Synthesis and Structural Characterization of a Dialuminum-Substituted Silicotungstate. The TBA salt of a dialuminum-substituted silicotungstate **1** was obtained by the reaction of the potassium salt of $[\gamma\text{-}SiW_{10}O_{36}]^{8-}$ (**SiW10**)[5] with 2 equiv of $Al(NO_3)_3$ with respect to **SiW10** in an acidic medium (see Experimental Section). The elemental analysis data showed that the Si:Al:W ratio in **1** was 1:2:10, respectively. Further, it was confirmed by the elemental analysis that no alkali metal cations of Na^+ and K^+ were found in **1** (<0.1 wt%). Compound **1** was soluble in various polar organic solvents such as CH_3CN, DMF, and DMSO, and the single crystals suitable for X-ray crystallographic analysis were successfully obtained by recrystallization in a mixed solvent of CH_3CN and water (see Experimental Section). The molecular structure is represented in Figure 1a and the selected bond lengths and angles are summarized in Table 1. The crystallographic data are summarized in Table S1, Supporting Information.

Three TBA cations per the anion were found in **1**. The bond valence sum (BVS) values of aluminum (3.14−3.19), tungsten (5.93−6.72), and silicon (3.65) indicate that the respective valences in **1** are +3, +6, and +4. Further, it was confirmed by the bond lengths that the axial positions of aluminum centers in **1** were occupied by water molecules and each aluminum center was linked by two μ-hydroxo ligands to form the $\{Al_2(\mu\text{-}OH)_2\}$ diamond core. The results of the BVS calculations, elemental analysis, and TG-DTA show that the formula of **1** is $TBA_3H[\gamma\text{-}SiW_{10}O_{36}\{Al(OH_2)\}_2(\mu\text{-}OH)_2]\cdot 4H_2O$. The formation of **1** anion is expressed by the following equation:

$$[\gamma\text{-}SiW_{10}O_{36}]^{8-} + 2Al^{3+} + 2H_2O \rightarrow [\gamma\text{-}SiW_{10}O_{36}Al_2(\mu\text{-}OH)_2]^{4-} + 2H^+ \quad (1)$$

As shown in Figure 1a, the anion part of **1** was a monomer of the dialuminum-substituted γ-Keggin silicotungstate. The axial positions of aluminum centers were occupied by aquo ligands, and the opposite axial positions were occupied by the oxygen atoms of the central $\{SiO_4\}$ unit with the average Al−O(Si) distance of 2.13 Å. Thus, the aluminum centers were in axially distorted octahedral environments, and the $\{Al_2(\mu\text{-}OH)_2\}$ diamond core was placed in the building pocket of **SiW10**.[6] The Al(1)−O(1), Al(1)−O(2), Al(2)−O(1), and Al(2)−O(2) bonds (average 1.85 Å) were almost equidistant. The average Al−O−Al and O−Al−O angles were 101.1° and 78.7°, respectively. The Al(1)···Al(2) distance in **1** was 2.863(1) Å. These bond lengths and angles were similar to that of the previously reported Salan complex with a similar dialuminum core.[7]

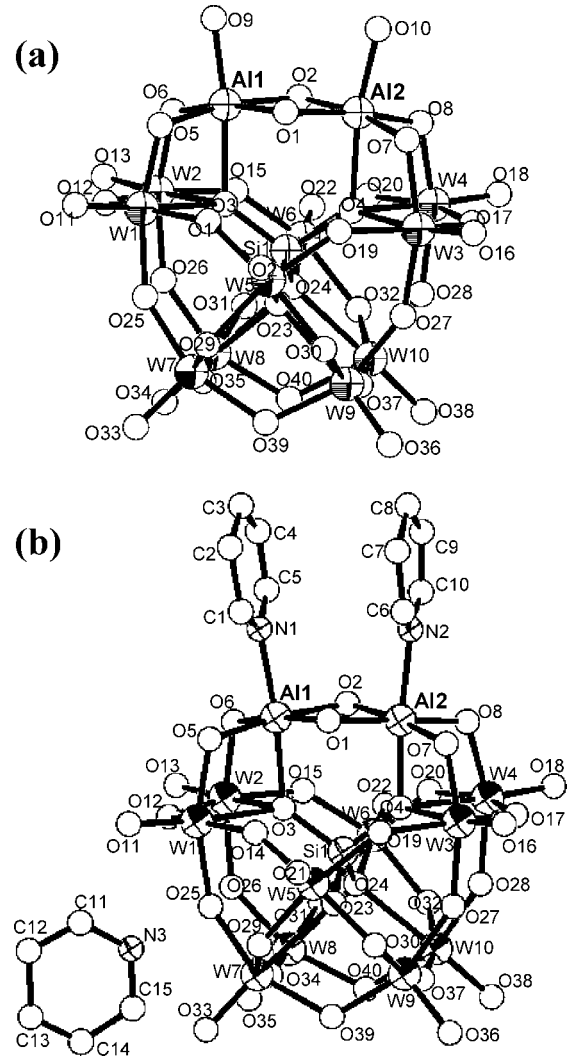

Figure 1. Molecular structures (ORTEP drawing) of (a) $TBA_3H[\gamma\text{-}SiW_{10}O_{36}\{Al(OH_2)\}_2(\mu\text{-}OH)_2]\cdot 4H_2O$ (**1**) and (b) $TBA_3[(C_5H_5N)H][\gamma\text{-}SiW_{10}O_{36}\{Al(C_5H_5N)\}_2(\mu\text{-}OH)_2]\cdot 2H_2O$ (**2**). TBA and water molecules (except for aquo ligands) were omitted for clarity.

As shown in Figure 2a, the ^{29}Si NMR spectrum of **1** showed a signal at −83.9 ppm, suggesting that **1** is a single species in the solvent. The ^{183}W NMR spectrum of **1** in CD_3CN showed three signals at −113.4, −119.2, and −139.4 ppm with the intensity ratio of 2:1:2, respectively (Figure 2b). The ^{183}W NMR spectrum of **1** in a mixed solvent of CD_3CN and DMSO-d_6 showed three signals at −72.1, −124.8, and −132.8 ppm with the intensity ratio of 2:1:2, respectively (Figure 2c). These results suggest that the cluster framework of **1** maintains the γ-Keggin

(4) (a) Zonnevijlle, F.; Tourné, C. M.; Tourné, G. F. *Inorg. Chem.* **1982**, *21*, 2742. (b) Liu, J.; Ortéga, F.; Sethuraman, P.; Katsoulis, D. E.; Costello, C. E.; Pope, M. T. *J. Chem. Soc., Dalton Trans.* **1992**, 1901. (c) Chen, Y.-G.; Qu, L. Y.; Peng, J.; Yu, M.; Lin, Y.-H.; Yu, Z.-L. *Jiegon Huaxue* **1993**, *12*, 338. (d) Yang, Q. H.; Zhou, D. F.; Dai, H. C.; Liu, J. F.; Xing, Y.; Lin, Y. H.; Jia, H. Q. *Polyhedron* **1997**, *16*, 3985. (e) Cowan, J. J.; Bailey, A. J.; Heintz, R. A.; Do, B. T.; Hardcastle, K. I.; Hill, C. L.; Weinstock, I. A. *Inorg. Chem.* **2001**, *40*, 6666. (f) Maksimov, G. M.; Fedotov, M. A. *Russ. J. Inorg. Chem.* **2001**, *46*, 327. (g) Casey, W. H. *Chem. Rev.* **2006**, *106*, 1. (h) Wang, J.; Yan, L.; Qian, G.; Li, S.; Yang, K.; Liu, H.; Wang, X. *Tetrahedron* **2007**, *63*, 1826.

(5) (a) Canny, J.; Tézé, A.; Thouvenot, R.; Hervé, G. *Inorg. Chem.* **1986**, *25*, 2114. (b) Tézé, A.; Hervé, G. *Inorg. Synth.* **1990**, *27*, 85.

(6) (a) Zhang, X.-Y.; O'Conner, C. J.; Jameson, G. B.; Pope, M. T. *Inorg. Chem.* **1996**, *35*, 30. (b) Cadot, E.; Béreau, V.; Marg, B.; Halut, S.; Sécheresse, F. *Inorg. Chem.* **1996**, *35*, 3099. (c) Nakagawa, Y.; Uehara, K.; Mizuno, N. *Inorg. Chem.* **2005**, *44*, 9068.

(7) Wei, P.; Atwood, D. A. *Polyhedron* **1999**, *18*, 641.

Table 1. Selected Bond Lengths (Å) and Angles (deg) in **1** and **2**

1		2	
	Lengths		
Al(1)···Al(2)	2.863(1)	Al(1)···Al(2)	2.832(8)
Al(1)−O(1)	1.841(19)	Al(1)−O(1)	1.819(19)
Al(1)−O(2)	1.88(2)	Al(1)−O(2)	1.87(2)
Al(2)−O(1)	1.837(19)	Al(2)−O(1)	1.906(19)
Al(2)−O(2)	1.85(2)	Al(2)−O(2)	1.84(2)
Al(1)−O(9)	1.869(18)	Al(1)−N(1)	2.033(17)
Al(2)−O(10)	1.859(19)	Al(2)−N(2)	2.061(18)
$Al-O_{W\ av}$	1.850	$Al-O_{W\ av}$	1.83
$Al-O_{Si\ av}$	2.125	$Al-O_{Si\ av}$	2.02
$W-O_{Si\ av}$	2.326	$W-O_{Si\ av}$	2.35
$W=O_{W\ av}$	1.710	$W=O_{W\ av}$	1.71
$W-O_{Al\ av}$	1.864	$W-O_{Al\ av}$	1.83
$W-O_{W\ av}$	1.919	$W-O_{W\ av}$	1.92
$Si-O_{av}$	1.659	$Si-O_{av}$	1.63
O(9)−O(10)	3.54(2)	N(1)−N(2)	3.47(2)
		$Py\cdots Py_{av}$	3.64
		N(3)−O(25)	2.84(3)
	Angles		
Al(1)−O(1)−Al(2)	102.2(9)	Al(1)−O(1)−Al(2)	99.0(9)
Al(1)−O(2)−Al(2)	100.0(9)	Al(1)−O(2)−Al(2)	99.6(9)
O(1)−Al(1)−O(2)	78.2(8)	O(1)−Al(1)−O(2)	80.5(8)
O(1)−Al(2)−O(2)	79.1(8)	O(1)−Al(2)−O(2)	79.1(8)
O(1)−Al(1)−O(9)	95.7(8)	O(1)−Al(1)−N(1)	92.7(8)
O(2)−Al(1)−O(9)	94.7(8)	O(2)−Al(1)−N(1)	92.8(9)
O(1)−Al(2)−O(10)	96.3(8)	O(1)−Al(2)−N(2)	94.2(8)
O(2)−Al(2)−O(10)	95.3(8)	O(2)−Al(2)−N(2)	87.8(8)
O(5)−Al(1)−O(9)	94.3(8)	O(5)−Al(1)−N(1)	91.9(8)
O(6)−Al(1)−O(9)	97.9(8)	O(6)−Al(1)−N(1)	95.0(9)
O(7)−Al(2)−O(10)	93.2(8)	O(7)−Al(2)−N(2)	92.9(8)
O(8)−Al(2)−O(10)	92.9(8)	O(8)−Al(2)−N(2)	91.4(7)
O(5)−Al(1)−O(6)	90.3(8)	O(5)−Al(1)−O(6)	92.8(8)
O(7)−Al(2)−O(8)	94.1(8)	O(7)−Al(2)−O(8)	92.3(8)
O(1)−Al(1)−O(5)	94.9(8)	O(1)−Al(1)−O(5)	92.3(9)
O(2)−Al(1)−O(6)	94.9(9)	O(2)−Al(1)−O(6)	93.8(9)
O(1)−Al(2)−O(7)	93.7(9)	O(1)−Al(2)−O(7)	95.2(9)
O(2)−Al(2)−O(8)	91.9(9)	O(2)−Al(2)−O(8)	93.3(9)
O(3)−Al(1)−O(9)	172.4(8)	O(3)−Al(1)−N(1)	173.0(7)
O(4)−Al(2)−O(10)	169.9(8)	O(4)−Al(2)−N(2)	172.2(8)

structure with the C_{2v} symmetry in these solution. The downfield shift and broadening of one set of tungsten signals in a mixed solvent of CD_3CN and DMSO-d_6 (observed at −72.1 ppm) are likely due to the coordination of DMSO-d_6 to the aluminum (Lewis acid) centers.

Reaction of Compound 1 with Bases (OH^- and Pyridine). As shown in Figure 3, a potentiometric titration of **1** with tetra-*n*-butylammonium hydroxide (TBAOH)[8] showed an inflection point at 1.0 ± 0.2 equiv of OH^- with respect to **1**, showing that complex **1** possesses one titratable proton ($[H^+]/[\mathbf{1}] = 1$). Therefore, the hydroxyl groups of the $\{Al_2(\mu\text{-}OH)_2\}$ core in **1** are not acidic enough to react with TBAOH.

Compound **1** was dissolved in CH_3CN, and the successive addition of pyridine yielded the single crystals (**2**, see Experimental Section). The elemental analysis suggests that three pyridine molecules are included in compound **2**. In the IR spectrum of **2**, the characteristic absorption bands of pyridine molecules coordinated to acidic sites were observed, and the bands at 1452 and 1540 cm^{-1} are assignable to pyridine molecules coordinated to Lewis acid and Brønsted acid (pyridinium cation) sites, respectively (Figure 4).[9] The molar ratio of (pyridine coordinated to Lewis acid sites)/(pyridinium cation) was calculated to be 2 by using the reported integrated molar extinction coefficients.[9]

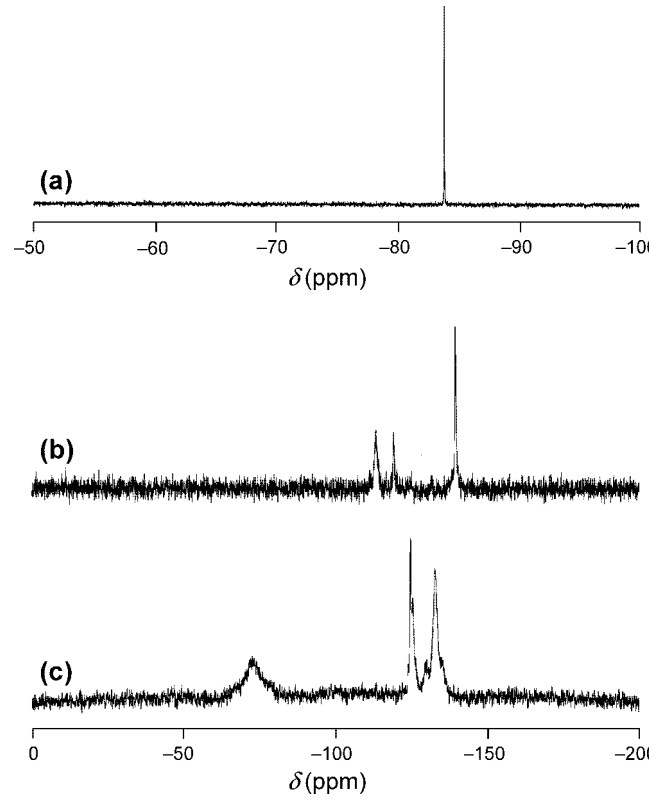

Figure 2. (a) ^{29}Si NMR spectrum of **1** in CD_3CN/DMSO-d_6 (2:1 v/v); (b) ^{183}W NMR spectrum in CD_3CN; (c) ^{183}W NMR spectrum in CD_3CN/DMSO-d_6 (2:1 v/v).

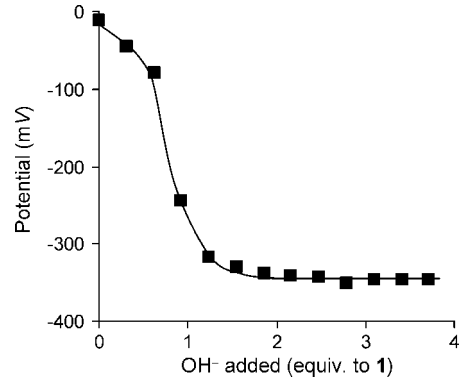

Figure 3. Profile for the potentiometric titration of **1** (0.05 mmol) in a mixed solvent of DMF and water (50 mL, 9:1 v/v) with 40% aqueous TBAOH as a titrant. The potentials are relative to a standard Ag/AgCl electrode.

The solid-state ^{15}N CPMAS NMR spectrum of **2** with ^{15}N-enriched pyridine showed signals assignable to pyridine coordinated to the aluminum centers (236.5 and 241.8 ppm) and pyridinium cation (183.2 ppm) (Figure 5).[10] Also, the ^{15}N NMR spectrum of the CD_3CN solution of **1** and ^{15}N-enriched pyridine (3 equiv with respect to **1**, 32 °C) showed signals assignable to pyridine coordinated to the aluminum centers (258.3 and 260.8 ppm).[10] These signal positions were very close to those of the

(8) Weiner, H.; Aiken, J. D., III; Finke, R. G. *Inorg. Chem.* **1996**, *35*, 7905.
(9) Emeis, C. A. *J. Catal.* **1993**, *141*, 347.
(10) (a) Maciel, G. E.; Haw, J. F.; Chuang, I.-S.; Hawkins, B. L.; Early, T. A.; McKay, D. R.; Petrakis, L. *J. Am. Chem. Soc.* **1983**, *105*, 17. (b) Ripmeester, J. A. *J. Am. Chem. Soc.* **1983**, *105*, 2925.

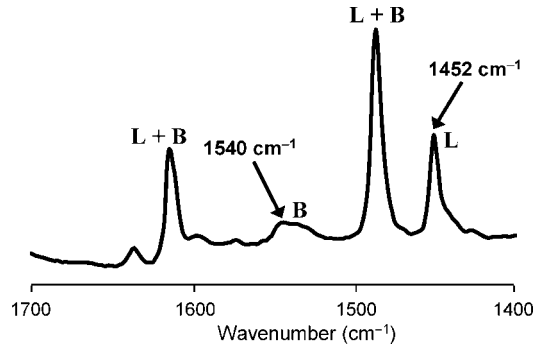

Figure 4. IR spectrum of pyridine molecules on **2**. The spectrum was obtained by subtracting the spectrum of **1** from that of **2**. L = pyridine molecules on Lewis acidic sites (Al centers), B = pyridine molecules on Brønsted acidic sites (pyridinium cations).

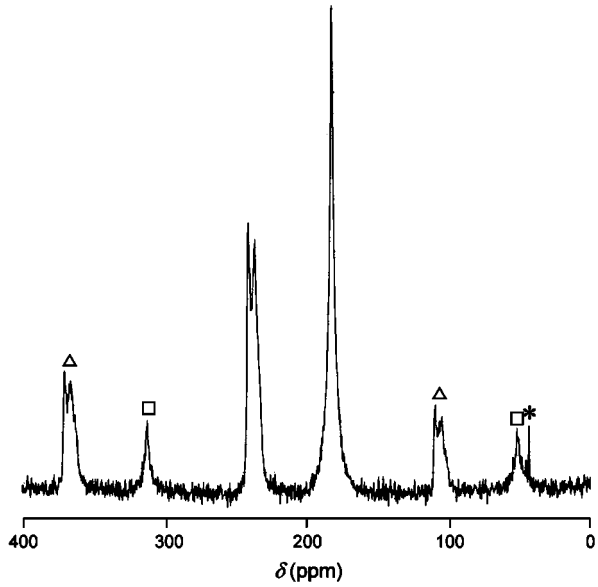

Figure 5. Solid-state ^{15}N CPMAS NMR spectrum of compound **2** obtained with ^{15}N-enriched pyridine. The triangles and squares indicate the spinning side bands of the signals due to pyridine coordinated to the aluminum centers (236.5 and 241.8 ppm) and pyridinium cation (183.2 ppm), respectively. The asterisk indicates the signal due to tetra-*n*-butylammonium.

solid-state NMR spectrum of **2**. In addition to these signals, a signal assignable to pyridine interacting with proton was observed at 300.2 ppm. Judging from the small upperfield shift from free pyridine ($\Delta\delta$ = 16.8 ppm), compound **1** likely acts as a weak proton donor in CD_3CN.[11]

We successfully obtained the high quality single crystals of **2** and the molecular structure could be determined by the X-ray crystallographic analysis. The molecular structure is represented in Figure 1b and the selected bond lengths and angles are summarized in Table 1. The crystallographic data are summarized in Table S1. As shown in Figure 1b, complex **2** was a monomer of the dialuminum-substituted γ-Keggin silicotungstate with three pyridine molecules. The BVS values of oxygen atoms O(1) (1.14) and O(2) (1.15) in **2** indicate that two aluminum atoms are also linked by two μ-hydroxo ligands to form the $\{Al_2(\mu\text{-}OH)_2\}$ diamond core. As expected from the IR and solid-state ^{15}N CPMAS NMR spectra of **2**, two of three pyridine molecules existed on the axial positions of aluminum centers and one of them existed as a pyridinium cation. The distance between the two pyridine molecules on the aluminum centers was 3.64 Å, and they are likely stabilized by the $\pi-\pi$ interaction. The strong hydrogen-bonding interaction between the pyridinium cation near the **SiW10** framework and O(25) atom was observed ($d_{N(3)-O(25)}$ = 2.84 Å). All these results indicate that complex **1** possesses two Lewis acid sites (aluminum centers) and one Brønsted acid (H^+) site.

Diastereoselective Cyclization of Citronellal Derivatives. Next, the cyclization of (+)-citronellal (**3**)[12] was carried out with the dialuminum-substituted silicotungstate **1**. Generally, the cyclization shows a complex selectivity pattern since **3** can be converted into four different diastereoisomers. The important feature of the cyclization is the diastereoselectivity toward (−)-isopulegol (**3a**), which is readily hydrogenated to the industrially important (−)-menthol.[12] Thus, the development of efficient catalysts that can diastereoselectively produce **3a** is very attractive. Typically, high diastereoselectivities to **3a** (ca. 60−80%) have been observed in the presence of Lewis acids.[13] With Brønsted acids, the diastereoselectivities are lower (ca. 50−70%) than those with Lewis acids.[14] There are only a few reports on the catalytic cyclization with ≥90% diastereoselectivity to **3a**.[13b,n−p]

Compound **1** showed high catalytic activity and selectivity for the cyclization of (+)-citronellal (**3**) and gave the corresponding isopulegol isomers (**3a**−**3d**) in high yields (Table 2). In this case, no etherification and dehydration, which are frequently observed in the Brønsted acid catalyzed reactions,[14] was observed. Under the same reaction conditions, no cyclization proceeded in the absence of the catalysts or in the presence

(11) Haslinger, E.; Schlederer, M.; Robien, W.; Wolschann, P. *Monatsh. Chem.* **1984**, *115*, 1345.

(12) (a) Pybus, D. H.; Sell, C. S. *The Chemistry of Fragrances*; RSC Paperbook: Cambridge, 1999. (b) da Silva Rocha, K. A.; Robles-Dutenhefner, P. A.; Sousa, E. M. B.; Kozhevnikova, E. F.; Kozhevnikov, I. V.; Gusevskaya, E. V. *Appl. Catal., A* **2007**, *317*, 171. (c) Lenardão, E. J.; Botteselle, G. V.; de Azambuja, F.; Perin, G.; Jacob, R. G. *Tetrahedron* **2007**, *63*, 6671.

(13) (a) Nakatani, Y.; Kawashima, K. *Synthesis* **1978**, 147. (b) Aggarwal, V. K.; Vennall, G. P.; Davey, P. N.; Newman, C. *Tetrahedron Lett.* **1998**, *39*, 1997. (c) Kočovskỳ, P.; Ahmed, G.; Šrogl, J.; Malkov, A. V.; Steele, J. *J. Org. Chem.* **1999**, *64*, 2765. (d) Milone, C.; Gangemi, C.; Neri, G.; Pistone, A.; Galvagno, S. *Appl. Catal., A* **2000**, *199*, 239. (e) Milone, C.; Perri, A.; Pistone, A.; Neri, G.; Galvagno, G. *Appl. Catal., A* **2002**, *233*, 151. (f) Corma, A.; Renz, M. *Chem. Commun.* **2004**, 550. (g) Andeade, C. K. Z.; Vercillo, O. E.; Rodrigues, J. P.; Silveira, D. P. *J. Braz. Chem. Soc.* **2004**, *15*, 813. (h) Anderson, E. D.; Ernat, J. J.; Nguyen, M. P.; Palma, A. C.; Mohan, R. S. *Tetrahedron Lett.* **2005**, *46*, 7747. (i) Alaerts, L.; Séguin, E.; Poelman, H.; Thibault-Starzyk, F.; Jacobs, P. A.; De Vos, D. E. *Chem. Eur. J.* **2006**, *12*, 7353. (j) Ramanathan, A.; Klomp, D.; Peters, J. A.; Hanefeld, U. *J. Mol. Catal. A* **2006**, *260*, 62. (k) Imachi, S.; Owada, K.; Onaka, M. *J. Mol. Catal. A* **2007**, *272*, 174. (l) Yoshida, A.; Hikichi, S.; Mizuno, N. *J. Organomet. Chem.* **2007**, *692*, 455. (m) Kikukawa, Y.; Yamaguchi, S.; Tsuchida, K.; Nakagawa, Y.; Uehara, K.; Yamaguchi, K.; Mizuno, N. *J. Am. Chem. Soc.* **2008**, *130*, 5472. (n) Tateiwa, J.; Kimura, A.; Takasuka, M.; Uemura, S. *J. Chem. Soc., Perkin Trans. 1* **1997**, 2169. (o) Iwata, T.; Okeda, Y.; Hori, Y. European Patent Application, EP 1 225 163 A2, 2002. (p) Yongzhong, Z.; Yuntong, N.; Jaenicke, S.; Chuah, G. K. *J. Catal.* **2005**, *229*, 404.

(14) (a) Fuentes, M.; Magraner, J.; De Las Pozas, C.; Roque-Malherbe, R.; Pariente, J. P.; Corma, A. *Appl. Catal.* **1989**, *47*, 367. (b) Laurent, R.; Laporterie, A.; Dubac, J.; Berlan, J.; Lefeuvre, S.; Audhuy, M. *J. Org. Chem.* **1992**, *57*, 7099. (c) Kropp, P. J.; Breton, G. W.; Craig, S. L.; Crawford, S. D.; Durland, W. F., Jr; Jones, J. E.; Raleigh, J. S. *J. Org. Chem.* **1995**, *60*, 4146. (d) Chuah, G. K.; Liu, S. H.; Jaenicke, S.; Harrison, L. J. *J. Catal.* **2001**, *200*, 352. (e) da Silva, K. A.; Robles-Dutenhefner, P. A.; Sousa, E. M. B.; Kozhevnikova, E. F.; Kozhevnikov, I. V.; Gusevskaya, E. V. *Catal. Commun.* **2004**, *5*, 425. (f) Mäki-Arvela, P.; Kumar, N.; Nieminen, V.; Sjöholm, R.; Salmi, T.; Murzin, D. Y. *J. Catal.* **2004**, *225*, 155. (g) Williams, J. T.; Bahia, P. S.; Kariuki, B. M.; Spencer, N.; Philp, D.; Snaith, J. S. *J. Org. Chem.* **2006**, *71*, 2460.

Table 2. Intramolecular Cyclization of **3**[a]

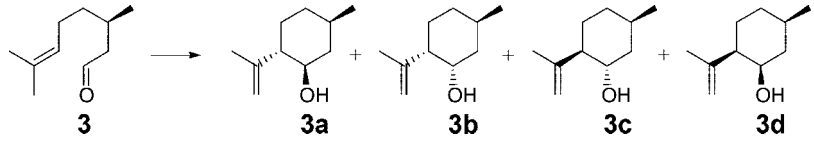

3 **3a** **3b** **3c** **3d**

				isomer ratio (%)			
catalyst	temp (°C)	time (h)	yield[b] (%)	**3a**	**3b**	**3c**	**3d**
1	75	10	93	**87**	9	nd	4
1	32	24	74	**88**	9	nd	3
1[c]	32	24	58	**91**	6	nd	3
2	32	24	nr	nd	nd	nd	nd
SiW10[d]	75	10	nr	nd	nd	nd	nd
$Al(NO)_3$[e]	75	10	30[f]	75	19	1	5
Hf4[g]	75	10	17	80	16	1	3
none	75	10	nr	nd	nd	nd	nd

[a] Reaction conditions: **3** (1 mmol), catalyst (2.5 mol %), acetonitrile (3 mL), Ar atmosphere. The yield and diastereoselectivity were determined by GC analysis using an internal standard. [b] Total yield of isopulegol isomers **3a**−**3d**. In the case of **1**-catalyzed cyclization, the selectivity toward isomers was >99% in all cases. [c] In the presence of 3 equiv of 2,6-lutidine. [d] TBA salt. [e] 5 mol %. [f] 70% selectivity. nr = no reaction. nd = not detected. [g] Cesium crown ether clathrate salts of $[(\gamma\text{-}SiW_{10}O_{36})_2\{Hf(H_2O)\}_4(\mu_4\text{-}O)(\mu\text{-}OH)_6]^{8-}$ (see ref 13m).

of **SiW10**. The **1**-catalyzed cyclization of **3** proceeded with high diastereoselectivity toward **3a** (87−91%), and *these values were the highest level* among those with previously reported systems (33−99%) (Table S2, Supporting Information).[13,14] The reaction rate for the **1**-catalyzed cyclization of **3** at 75 °C was 134 mM h^{-1} and 24 times higher than that with the tetra-nuclear hafnium containing polyoxometalate $[(\gamma\text{-}SiW_{10}O_{36})_2\{Hf(H_2O)\}_4(\mu_4\text{-}O)(\mu\text{-}OH)_6]^{8-}$ (**Hf4**) under the same reaction conditions (5.6 mM h^{-1}).[13m] In addition, the diastereoselectivity toward **3a** in the presence of **1** (87%) was higher than that in the presence of **Hf4** (80%).[13m] The reaction profile for the **1**-catalyzed cyclization of **3** shows that the diastereoselectivities toward **3a** were always around 90% at 0−99% conversions of **3a**, showing that no interconversion of these isomers (e.g., retro-ene reaction) proceeds under the present conditions. In addition, the reaction of 3-methylcitronellal (**4**) proceeded diastereoselectively to give *trans* isomer as a major product (eq 2).

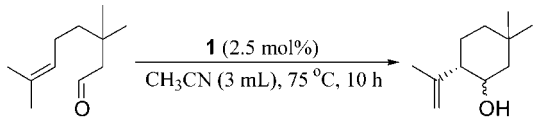

(2)

4 (1 mmol)
conv. >99%

total yield >99% (*trans*:*cis* = 98:2)

To clarify the active sites for the cyclization, the **1**-catalyzed cyclization of **3** in the presence of pyridine or 2,6-lutidine was carried out (Figure 6). Pyridine can interact with both Brønsted and Lewis acid sites via protonation and coordination, respectively.[15] In contrast, it is well-known that 2,6-lutidine can selectively interact with Brønsted acid sites and can not interact with Lewis acid sites due to the steric hindrance.[15] It was also confirmed by the molecular modeling that 2,6-lutidine cannot approach to the Lewis acid sites (aluminum centers in **1**), but pyridine can approach to the sites (Figure S1, Supporting Information). As shown in Figure 6, the reaction rate decreased with an increase in the amount of pyridine added and the cyclization hardly proceeded in the presence of 2 equiv of pyridine with respect to **1**. On the other hand, the reaction rate

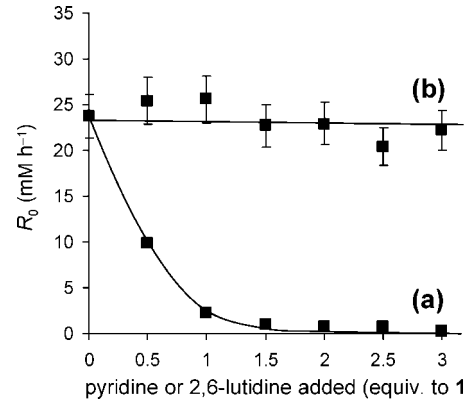

Figure 6. Rates for cyclization of **3** as a function of the amount of bases added: (a) pyridine and (b) 2,6-lutidine.

(22.2 mM h^{-1}) and diastereoselectivity (91%) to **3a** even in the presence of 3 equiv of 2,6-lutidine were almost the same as those in the absence (23.7 mM h^{-1}, 88%).

The above-mentioned results show that the present cyclization is mainly promoted by the Lewis acid sites (aluminum centers) in **1**. The electrostatic potential (ESP) around **1** also supports the idea.[16] Thus, the cyclization proceeds via the Lewis acid catalyzed carbonyl-ene-type mechanism.[13] A possible reaction mechanism for the present cyclization is given in Scheme S1, Supporting Information. The coordination of **3** to the Lewis acid center leads to four possible transition states shown in Figure 7a to produce the corresponding isopulegol isomers. It is likely that the energies at the transition states are much dependent on the kinds of the Lewis acids (steric and electronic effects).[13] In order to clarify the origin of the high diastereoselectivity (isomer ratio) for the **1**-catalyzed cyclization of **3**, the energies at the

(15) (a) Brown, H. C.; Johannesen, R. B. *J. Am. Chem. Soc.* **1953**, *75*, 16. (b) Murell, L. L.; Dispenziere, N. C., Jr *J. Catal.* **1989**, *117*, 275. (c) Corma, A. *Chem. Rev.* **1995**, *95*, 559.

(16) (a) We calculated the ESP around **1** from electron densities with B3LYP level theory. The topology of ESPs has proved to be very useful for detecting the most basic regions of polyoxometalates. López, X.; Bo, C.; Poblet, J. M. *J. Am. Chem. Soc.* **2002**, *124*, 12574. (b) Nucleophilic species (citronellal derivatives) would approach to the polyoxometalate molecule along a path where the ESP is as high as possible. For compound **1**, the regions close to the axial sites of the aluminum centers (the ESP value at the saddle point = −0.28 hartree/e) were calculated to be more electrophilic (acidic) than the other sites including bridged μ-OH groups and the polyoxotungstate regions (< −0.30 hartree/e).

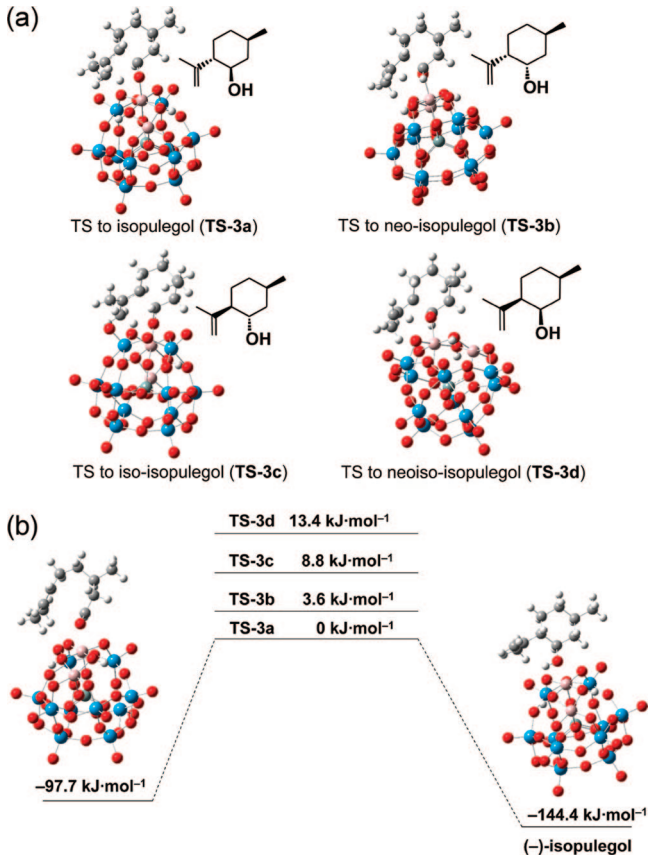

Figure 7. (a) Calculated structures of transitions states to produce isopulegol isomers for the **1**-catalyzed cyclization of **3**; (b) energy diagram.

transition states were estimated by DFT calculations at the B3LYP level theory (see Experimental Section). The transition state to produce **3a** (**TS-3a**) was at least by 3.6 kJ mol^{-1} more stable than the other three transition states (Figure 7b), showing that the formation of the transition state **TS-3a** is sterically and electronically more favorable than the others in the **1**-catalyzed cyclization of **3**.[17] Therefore, the diastereoselectivity toward different isopulegol isomers for the present **1**-catalyzed cyclization of **3** can be explained by the stability of the corresponding transition states.

Conclusion

The novel dialuminum-substituted silicotungstate **1** has been synthesized and the molecular structure was successfully determined. Compound **1** could act as an efficient homogeneous Lewis acid catalyst for the cyclization of citronellal derivatives with the high chemo- and diastereoselectivity.

Experimental Section

General. IR spectra were measured on Jasco FT/IR-460 Plus. A mixture of the aluminum-substituted polyoxometalate (**1** or **2**) and KBr was pressed into the disk with a radius of 10 mm, and the spectrum was recorded at room temperature (ca. 20 °C). The difference spectrum (Figure 4) was obtained by subtracting the spectrum of **1** from that of **2**. The ratio of pyridine adsorbed on Lewis and Brønsted acid sites were determined by using the following integrated molar extinction coefficients: 2.22 and 1.67 cm μmol^{-1} for Lewis (1452 cm^{-1}) and Brønsted acid sites (1540 cm^{-1}), respectively.[9] Liquid-state NMR spectra were recorded on JEOL JNM-EX-270. ^{1}H and $^{13}C\{^{1}H\}$ NMR spectra (internal standard: TMS, 0 ppm) were measured at 270 and 67.8 MHz, respectively. ^{15}N (external standard CH_3NO_2, 379.8 ppm[18]), ^{27}Al (external standard $Al(NO_3)_3$, 0 ppm), ^{29}Si (external standard TMS, 0 ppm), and ^{183}W NMR spectra (external standard Na_2WO_4, 0 ppm) were measured at 27.2, 70.0, 53.5, and 11.2 MHz, respectively. Solid-state ^{15}N CPMAS NMR spectrum of **2** obtained with ^{15}N-enriched pyridine (MAS rate = 4 kHz) was recorded on Chemagnetics CMX-300 Infinity spectrometer operating at 30.5 MHz. The repetition time was 3 s, and the cross-polarization contact time was 5 ms. NH_4NO_3 (nitrate at 353.7 ppm[19]) was used as an external standard for the calibration of chemical shifts. The potentiometric titration of **1** (0.05 mmol) was carried out in a mixed solvent of DMF and water (50 mL, 9:1 v/v) with 40% aqueous tetra-*n*-butylammonium hydroxide (TBAOH) as a titrant.[8] Diffraction measurements were made on a Rigaku AFC-10 Saturn 70 CCD detector with graphite monochromated Mo Kα radiation (λ = 0.71069 Å) at 153 K. Data were collected and processed using CrystalClear[20] for Windows software and HKL2000[21] for Linux software. Neutral scattering factors were obtained from the standard source. In the reduction of data, Lorentz and polarization corrections were made. The structural analysis was performed using CrystalStructure[22] and Win-GX for Windows software.[23] All structures were solved by SHELXS-97 (direct methods) and refined by SHELXH-97.[24]

$Na_2WO_4 \cdot 2H_2O$, $Na_2SiO_3 \cdot 9H_2O$, and aluminum salts were obtained from Wako, Kanto, or Nacalai (reagent grade) and used as received. The dilacunary precursor of $K_8[\gamma\text{-}SiW_{10}O_{36}] \cdot 12H_2O$ was synthesized according to ref 5b. (+)-Citronellal (**3a**) and solvents were obtained from TCI (reagent grade) and were carefully purified before the use.[25] ^{15}N-Enriched pyridine was obtained from Aldrich (^{15}N > 98%) and was used as received. 3-Methylcitronellal (**4a**) was synthesized by the reaction of citral with cuprate.[26]

Synthesis of Compound 1. Compound **1** was synthesized as follows. $K_8[\gamma\text{-}SiW_{10}O_{36}] \cdot 12H_2O$ (10.0 g, 3.4 mmol) was dissolved in deionized water (100 mL). Then, $Al(NO_3)_3 \cdot 9H_2O$ (2.6 g, 6.9 mmol) was added in a single step, and the pH of the solution was adjusted to 3.8 with an aqueous K_2CO_3 solution (2.0 M). After 15 min, $[(CH_3)_4N]Cl$ (4.8 g, 44 mmol) was added to the solution in a single step followed by stirring for 30 min at room temperature (ca. 20 °C). The white precipitate of the tetramethylammonium salt was collected by filtration and washed with a small amount of water and diethylether (7.0 g). The tetramethylammonium salt was dissolved in deionized water (250 mL). Then, $[(C_4H_9)_4N]Br$ (28.0 g, 87.3 mmol) was added to the solution in a single step, and the pH of the solution was adjusted to 2.6 with an aqueous HNO_3 solution (1.0 M). The white precipitate of TBA salt (**1**) was collected by filtration and washed with a small amount of water and diethylether. The crude product was purified with the precipitation method (addition of 1.0 L of water into 50 mL of a CH_3CN solution

(17) The Boltzmann distribution of these transition states (**TS-3a**:**TS-3b**:**TS-3c**:**TS-3d** = 78:19:2:<1 (at 32 °C)) was fairly agreed with the isomer ratio for the present cyclization (Table S3, Supporting Information).

(18) Wishart, D. S.; Bigam, C. G.; Yao, J.; Abildgaard, F.; Dyson, H. J.; Oldfield, E.; Markley, J. L.; Sykes, B. D. *J. Biomol. NMR* **1995**, *6*, 135.
(19) Ripmeester, J. A. *J. Am. Chem. Soc.* **1983**, *105*, 2925.
(20) (a) *CrystalClear* 1.3.6; Rigaku and Rigaku/MSC: The Woodlands, TX. (b) Pflugrath, J. W. *Acta Crystallogr.* **1999**, *D55*, 1718.
(21) Otwinowski, Z.; Minor, W. Processing of X-ray Diffraction Data Collected in Oscillation Mode. In *Methods in Enzymology*; Carter, C. W., Jr.; Sweet, R. M., Eds.; Macromolecular Crystallography, Part A; Academic Press: New York, 1997; Vol. 276, pp 307−326.
(22) *CrystalStructure* 3.8, Rigaku and Rigaku/MSC: The Woodlands, TX.
(23) Farrugia, L. J. *J. Appl. Crystallogr.* **1999**, *32*, 837.
(24) Sheldrick, G. M. *SHELX97, Programs for Crystal Structure Analysis*, Release 97-2; University of Göttingen: Göttingen, Germany, 1997.
(25) *Purification of Laboratory Chemicals*, 3rd ed.; Perrin, D. D., Armarego, W. L. F., Eds.; Pergamon Press: Oxford, 1988.
(26) (a) Sakane, S.; Maruoka, K.; Yamamoto, H. *Tetrahedron* **1986**, *42*, 2203. (b) Sakane, S.; Maruoka, K.; Yamamoto, H. *Tetrahedron Lett.* **1985**, *26*, 5535.

of the crude product), giving 4.9 g of the purified **1** (43% yield based on $K_8[\gamma\text{-}SiW_{10}O_{36}]\cdot 12H_2O$). The needle-like single crystals suitable for X-ray analysis were obtained by recrystallization in a mixed solvent of CH_3CN and water. Anal. Calcd for $[(n\text{-}C_4H_9)_4N]_3H[\gamma\text{-}SiW_{10}O_{36}\{Al(OH_2)\}_2(\mu\text{-}OH)_2]\cdot 4H_2O$: C, 17.12; H, 3.68; N, 1.25; Si, 0.83; W, 54.60; Al, 1.60. Found: C, 17.67; H, 3.60; N, 1.12; Si, 0.83; W, 54.90; Al, 1.60. IR (KBr pellet; 4000−400 cm^{-1}): 3433, 3221, 2962, 2935, 2974, 2734, 1628, 1483, 1463, 1381, 1364, 1347, 1308, 1282, 1252, 1152, 1106, 1058, 1028, 1001, 966, 905, 880, 865, 802, 627, 539, 488, 466, 411. ^{27}Al NMR (70.0 MHz, CD_3CN/DMSO-d_6 (2:1 v/v), 25 °C): δ 57.0. ^{29}Si NMR (53.5 MHz, CD_3CN/DMSO-d_6 (2:1 v/v), 25 °C): δ −83.9. ^{183}W NMR (11.2 MHz, CD_3CN/DMSO-d_6 (2:1 v/v), 25 °C) δ −72.1, −124.8, −132.8.

Synthesis of Compound 2. Compound **2** was synthesized as follows. Compound **1** (0.20 g, 59.4 μmol) was dissolved in a mixed solvent of CH_3CN and pyridine (0.4 mL/4.8 mL). The solution was kept at room temperature (ca. 20 °C) for 1 week, and colorless single crystals suitable for X-ray analysis appeared. The crystals were collected by filtration and washed with a small amount of CH_3CN (0.11 g, 52% yield based on **1**). Anal. Calcd for $[(n\text{-}C_4H_9)_4N]_3[(C_5H_5N)H][\gamma\text{-}SiW_{10}O_{36}\{Al(C_5H_5N)\}_2(\mu\text{-}OH)_2]\cdot 2H_2O$: C, 21.42; H, 3.71; N, 2.38; Si, 0.80; W, 52.10; Al, 1.53. Found: C, 21.58; H, 3.48; N, 2.50; Si, 0.84; W, 54.29; Al, 1.62. IR (KBr pellet; 4000−400 cm^{-1}): 3617, 3446, 3225, 3164, 3133, 3066, 2961, 2935, 2873, 2734, 1636, 1614, 1544, 1486, 1452, 1381, 1346, 1251, 1219, 1203, 1171, 1153, 1106, 1075, 1052, 997, 961, 907, 883, 821, 792, 710, 648, 621, 607, 545, 528, 508, 489, 474, 467, 453, 439, 414.

DFT Calculation. The calculations were carried out at the B3LYP level theory[27] with 6-31G* basis sets for H, C, O, Al, and Si atoms, and the double-ζ quality basis sets with effective core potentials proposed by Hay and Wadt[28] for W atoms. Transition state structures were searched by numerically estimating the matrix of second-order energy derivatives at every optimization step and by requiring exactly one eigenvalue of this matrix to be negative. The optimized geometries are shown in Figure 7a. The zero-point vibrational energies were not included. All calculations were performed with the Gaussian03 program package.[29]

Cyclization of Citronellal Derivatives. The catalytic cyclization was carried out with a glass tube reactor. All operations were carried out in a glovebox under Ar. Compound **1**, substrate, CH_3CN, and naphthalene (internal standard) were successively placed into a glass tube reactor. A Teflon-coated magnetic stir bar was added, and the reaction mixture was stirred (800 rpm) at 75 °C (or 32 °C) under Ar atmosphere. The yield, chemoselectivity, and diastereoselectivity were periodically determined by GC analysis. The products were confirmed by the comparison of GC retention times, mass spectra, and ^{1}H and ^{13}C NMR spectra with those of authentic samples.

Acknowledgment. This work was supported in part by the Core Research for Evolutional Science and Technology (CREST) program of the Japan Science and Technology Agency (JST), Global COE Program (Chemistry Innovation through Cooperation of Science and Engineering), and the Grants-in-Aid for Scientific Researches from Ministry of Education, Culture, Sports, Science and Technology.

Supporting Information Available: CIF files of **1** and **2**, Tables S1−S7, Figure S1 and Schemes S1 and S2, and complete ref 29. This material is available free of charge via the Internet at http://pubs.acs.org.

JA8014154

(27) Becke, A. D. *J. Chem. Phys.* **1993**, *98*, 1372.
(28) Hay, P. J.; Wadt, W. R. *J. Chem. Phys.* **1985**, *82*, 270.
(29) Frisch, M. J.; et al. *Gaussian 03* (Revision D.02); Gaussian, Inc.: Wallingford, CT, 2004.